Dispersion of Plasma Dust Acoustic Waves in the Strong-Coupling Regime

J. B. Pieper and J. Goree*

Department of Physics and Astronomy, The University of Iowa, Iowa City, Iowa 52242

(Received 21 June 1996)

Low-frequency compressional waves were observed in a suspension of strongly coupled 9.4 μm spheres in an rf Kr plasma. Both parts of the complex wave number were measured to determine the dispersion relation, which agreed with a theoretical model of damped dust acoustic waves, ignoring strong coupling, but not with a strongly coupled dust-lattice wave model. The results yield experimental values for the dust plasma frequency, charge, Debye length, and damping rate, and support the applicability of fluid-based dispersion relations to strongly coupled dusty plasmas, which has been a controversy. [S0031-9007(96)01326-9]

PACS numbers: 52.35.Fp, 52.25.Dg, 52.25.Vy

A dusty plasma is a three-component plasma consisting of electrons, ions, and massive solid particles held in suspension. The solid particles usually charge negatively to a large value [1]. The introduction of a third component allows new modes to propagate in the plasma. In particular, the dust acoustic wave (DAW) is analogous to the ion acoustic wave, but occurs at very low frequency [1–7]. Previous laboratory observations of wave motion in suspensions of small particles at frequencies of 10–15 Hz by Barkan, Merlino, and D'Angelo were attributed to the DAW [8].

A controversy has arisen whether modes such as the DAW derived theoretically from continuum-based models are applicable to laboratory dusty plasmas. These plasmas are generally strongly coupled, i.e., the coupling parameter is large, $\Gamma = q^2/4\pi\varepsilon_0\Delta k_B T \gg 1$ for particles separated by a typical distance Δ. This parameter is the ratio of the Coulomb potential and kinetic energies. Most commonly, plasmas are gaslike and weakly coupled ($\Gamma \ll 1$), and continuum models, which are derived from the BBGKY hierarchy by neglecting Coulomb interactions between discrete particles, are valid. Dust particles suspended in laboratory plasmas are visibly discrete, and often strongly coupled ($\Gamma \gg 1$). Recently Wang and Bhattacharjee (WB) expanded the BBGKY hierarchy for $\Gamma \gg 1$, and arrived again at the Vlasov equation [9], from which fluid equations are derived.

Here we present measurements of the dispersion relation of driven compressional waves in a strongly coupled dusty plasma in the parameter range $\lambda_D > \Delta \gg \lambda_{Dd}$ and $\Gamma \gg 1$. The DAW dispersion relation derived from a fluid model shows agreement with the experiment.

We produced a krypton plasma by applying a 13.55 MHz rf voltage to a horizontal Al electrode with a surface depression 1.5 mm deep and ~6 cm in diameter. Polymer spheres of diameter 9.4 ± 0.3 μm and density 1.51 g/cm^3 were shaken into the plasma region above the electrode, where they were levitated by the force balance between gravity and the electric field in the electrode's plasma sheath. The depression in the electrode surface acted as a lateral trap for the particles by producing a horizontal component of the electric field localized near its edges. The spheres were too massive to respond to the 13.55 MHz rf. The chamber walls acted as the second electrode, and at lower pressures (below 220 mTorr) we also used a grounded Al ring electrode 2.5 cm above the driven electrode. The Kr pressure was regulated at a small flow rate (1 SCCM) that caused no detectable disturbance of the particles. Experiments were repeated for four pressures. We adjusted the rf voltage and the number of particles in the cloud to attain the most ordered particle suspension possible at a given pressure; this is different from phase transition experiments reported by other authors who did not vary the rf voltage or particle count while varying the gas pressure [10].

To detect the waves, we illuminated particles by a horizontal sheet of laser light and imaged them with a video camera looking through the ring's opening down at the lower electrode. Details of the apparatus are presented elsewhere [11]. In the vertical direction, the particle cloud was three layers thick in the region where we made our measurements, and it had a simple-hexagonal structure [11]. Only one of the three layers was imaged at a time.

Analysis [12] of the equilibrium (without driven waves) revealed that the particles were arranged in an ordered structure. The structure was generally liquidlike, with six-fold particle coordination and short-range translational and orientational order. The orientational correlation length ξ_6 increased from about 2Δ at the lowest pressures to 14Δ at 300 mTorr, while the translational correlation length ξ was almost constant at $(2-3)\Delta$ over the pressure range.

To characterize the dust velocity distribution $f_d(v)$ at equilibrium, we imaged particles in a vertical (x-y) plane using a long-distance microscope. We found that $f_d(v)$ was anisotropic and Maxwellian, with a higher kinetic temperature (Table I) in the x-y plane, $k_B T_d^{xy} = \langle m v_x^2 \rangle$, than in the vertical direction, $k_B T_d^z = \langle m v_z^2 \rangle$. This is because the potential energy contribution to the temperature, which could not be measured, should have a deeper minimum in the vertical direction than in the horizontal, due to the vertical confining potentials. For

computing Γ, we will use the values of T_d for motion in the x-y plane only.

To drive an electrostatic wave, we used the scheme of Zuzic, Thomas, and Morfill [13] as shown in Fig. 1. An electrically isolated W wire of diameter 0.25 mm was stretched horizontally above the depressed electrode surface, at a height of 3–5 mm, which was adjusted in each experiment to be near the equilibrium particle height. To excite longitudinal waves in the particle cloud, the wire was driven by a sinusoidal voltage source of about 30 V peak to peak (p-p).

To avoid disturbing the plasma, the sinusoid was given a dc offset of -40 V relative to the chamber walls. Without the dc offset, a large electron current would be drawn during the positive half cycle of the ac voltage, whereas, with the negative offset, a much smaller ion current was drawn that varied little over the ac cycle. As a test, a Langmuir probe, which was dc coupled to an oscilloscope, was inserted into the plasma a few mm from the driven wire. We found that the probe's floating potential was modulated at the wire's frequency with an amplitude two decades smaller than at 13.55 MHz.

We recorded the particle motions on video tape. The driving frequency was varied in steps from 1 to 10 Hz. Later, we digitized 1 s (30 frame) segments of the recording [14]. Image-processing software yielded the coordinates of all the particle in an image. A given particle was tracked from one frame to the next through the 30-frame sequence by searching a frame in a rectangular area centered on a particle's position in the previous frame. Each particle's motion was separated into the time-averaged position $\langle x \rangle$ and the deviation $\delta x(t_k)$. The deviation was then averaged over the ignorable coordinate y, parallel to the wire and wave fronts, by binning particles in each frame t_k based on their average distance $\langle x \rangle$ from the wire. Finally, the averaged time-dependent deviations in each bin were assumed to have

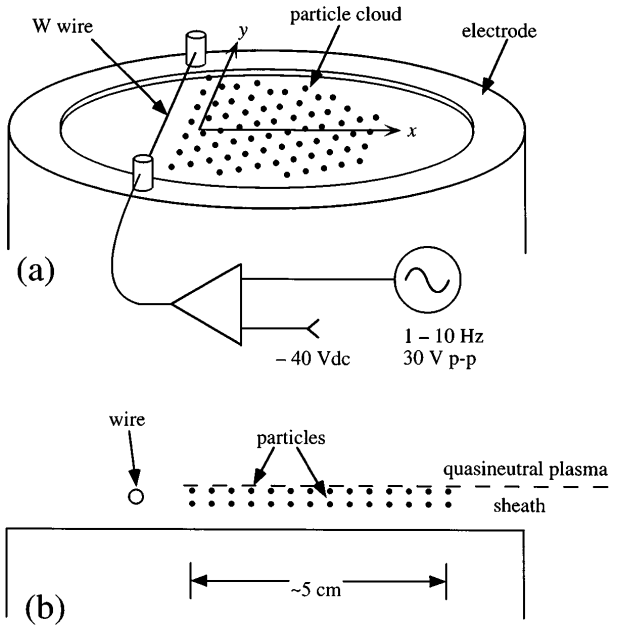

FIG. 1. Schematic diagram of the apparatus. (a) Perspective view of the electrode showing locations of the excitation wire and particles, the coordinate system, and the block diagram of the wave-driving electronics. (b) Side view showing particle location with respect to the electrode's sheath.

TABLE I. Experimental parameters at each Kr gas pressure. The rf electrode voltage $\nu_{\mathrm{rf,p\text{-}p}}$ was measured with an oscilloscope probe. Dust thermal energies $k_B T_d^{xy,z}$ were calculated from measurements of the random particle velocities. The average particle separation Δ was measured directly from the video images. The plasma frequency ω_{pd}, Debye length λ_D, and damping rate ν_{fit} were determined from the curve fits in Fig. 2. The orientational correlation length ξ_6 is from a fit to the correlation function $g_6(r)$ for the static structure. The experimental damping rate is compared with the value ν_{calc} calculated from Eq. (2.2) of Ref. [17], assuming a gas temperature of 300 K. The particle charge number Z and coupling parameter Γ were calculated from ω_{pd}, the particle density n_{d0}, and $k_B T_d^{xy}$.

	Gas pressure			
Parameter	55 mTorr	100 mTorr	220 mTorr	300 mTorr
Measured				
$\nu_{\mathrm{rf,p\text{-}p}}$ (V)	36	31	90	108
$k_B T_d^{xy}$ (eV)	1.1 ± 0.2	3.8 ± 0.3	0.024 ± 0.002	0.028 ± 0.002
$k_B T_d^{z}$ (eV)	0.039 ± 0.005	2.8 ± 0.3	0.0078 ± 0.0009	0.0036 ± 0.0004
Δ (mm)	0.58 ± 0.09	0.48 ± 0.05	0.29 ± 0.02	0.28 ± 0.02
Fit parameters				
$\omega_{pd}/2\pi$ (Hz)	3.2 ± 0.3	4.6 ± 0.2	9.0 ± 0.3	22 ± 5
λ_D (mm)	3.85 ± 0.15	2.56 ± 0.06	1.19 ± 0.03	0.46 ± 0.06
$\nu_{\mathrm{fit}}/2\pi$ (Hz)	3.9 ± 0.9	5.2 ± .7	9.0 ± 0.7	15.9 ± 3.4
ξ_6 (mm)	1.50 ± 0.08	0.98 ± 0.02	2.20 ± 0.04	3.80 ± 0.06
Computed				
$\nu_{\mathrm{calc}}/2\pi$ (Hz)	2.1	3.8	8.5	11.5
$Z\,(10^3)$	−3.8 ± 0.4	−3.8 ± 0.2	−3.4 ± 0.1	−7.2 ± 1.6
Γ	32 ± 8	11.4 ± 1.4	2400 ± 220	10 000 ± 4600
Δ/λ_D	0.15 ± 0.03	0.18 ± 0.02	0.24 ± 0.02	0.61 ± 0.12

the form $\delta x(t) = A\cos(\omega t - \varphi)$, where ω is the driving frequency. The amplitude A and phase φ were extracted by calculating the Fourier sum

$$\frac{2\omega}{n\pi}\sum_{k=1}^{N} x(t_k)\exp(i\omega t_k)\Delta t = A\exp(i\varphi), \qquad (1)$$

where n is the number of complete half cycles contained in the data set, N is the nearest integer to $n\pi/\omega\Delta t$, and $\Delta t = 1/30$ s. The sinusoid constructed from A and φ fit the data very accurately.

The charging time was 6 orders of magnitude faster than the wave oscillation, so that the charge on the particles might vary synchronously with fluctuations in the electron and ion densities [15]. Linear modifications of the real dispersion relation due to this effect are not expected, due to a small value, $P < 1$, of the dust density parameter [5]. Nonlinear effects due to large amplitudes were not observed. In tests of linearity, a full spectral analysis of the motion showed that harmonics of the drive frequency were typically 30 dB or more below the fundamental response, and the amplitude was found to scale proportionally with the peak-to-peak wire voltage.

To obtain the experimental dispersion relation k vs ω as shown in Fig. 2, we found both parts of the wave number $k = k_r + ik_i$ by fitting the amplitude and phase as functions of x to decaying-exponential and linear functions, respectively.

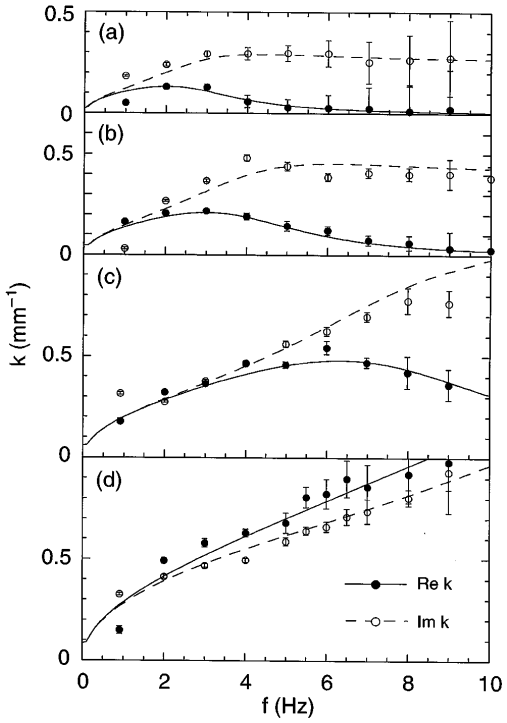

FIG. 2. Dispersion relation. Experimentally measured k_r (●) and k_i (○) of compressional waves in a Kr plasma are shown as a function of driving frequency for gas pressures of (a) 55, (b) 100, (c) 220, and (d) 300 mTorr. The curves represent fits by the theoretical DAW dispersion relation of Eq. (2). Free parameters (plasma frequency ω_{pd}, Debye length λ_D, and damping rate ν) are listed in Table I.

The imaginary part of k arises from neutral gas drag. The drag also cooled the particle thermal motion so the particles would be strongly coupled. Although k_i was often larger than k_r, the particle motion was always unambiguously wavelike, so our analysis was able to yield accurate measurements of k. The frequency is purely real since the mode was driven.

Analytical theory for the low-frequency compressional dispersion relation can be done easily in two extreme limits: a damped dust-lattice wave (DLW) [15] and a damped DAW. In the limit of $\Delta \gg \lambda_D$, particles in one dimension interact only with their two nearest neighbors through the shielded Coulomb potential. Expanding this potential about the equilibrium particle positions, particles in one dimension behave the same as a simple lattice of identical masses connected by springs. This yields a DLW dispersion relation where $k_r > k_i$ for all ω, and k_r increases linearly with ω in the high-frequency limit. This is not seen in the experimental results, where k_r rolls over at high frequencies. This rollover indicates a transition from a damped propagating wave to an evanescent wave, which does not occur in the DLW model.

A damped DAW, on the other hand, successfully fits the experimental measurements. This model assumes a continuum limit, $\Delta \gg \lambda_D$, and ignores particle discreteness. We follow Rao, Shukla, and Yu [2], but add a drag term $-mv\nu$ in the fluid momentum equation for dust, yielding the dispersion relation

$$k^2 = k_D^2\,\frac{\omega(\omega + i\nu)}{\omega_{pd}^2 - \omega(\omega + i\nu)}. \qquad (2)$$

This assumes charge neutrality, no dust motion in the equilibrium state, Boltzmann electron and ion responses, and a plane wave $\exp(ikx - i\omega t)$. Here ν is the damping rate, and $k_D = 1/\lambda_D = (\lambda_{De}^{-2} + \lambda_{Di}^{-2})^{1/2}$ is the total inverse Debye length, with λ_{De} and λ_{Di} the electron and ion Debye lengths $(\varepsilon_0 k_B T_{e,i}/n_{e,i}e^2)^{1/2}$. The dust Debye length is assumed to be negligible and does not enter into our expressions. The dust plasma frequency is $\omega_{pd} = (Z^2e^2n_{d0}/\varepsilon_0 m)^{1/2}$, where Z, m, and n_{d0} are the charge, mass, and number density of the dust. In the absence of damping, the wave number would be purely real, resonant ($k \to \infty$), and purely imaginary (evanescent) for $\omega < \omega_{pd}, \omega = \omega_{pd}, \omega > \omega_{pd}$, respectively. With strong damping, the dispersion does not have this discontinuity at the plasma frequency.

The real and imaginary parts of Eq. (2) were fitted to the experimental data. These fits are shown along with the data in Fig. 2. The free parameters k_D, ω_{pd}, and ν had the same trial values in the simultaneous real and imaginary fits. The results are given in Table I, including ν calculated for Epstein drag with diffuse scattering of gas molecules from spherical particles [16,17], the particle charge Z, and coupling parameter Γ. The last two quantities were calculated from ω_{pd} using the measured dust kinetic temperature T_d^{xy} and particle separation Δ, and the value of the three-dimensional dust density n_{d0}

was obtained from the measured two-dimensional density and spacing between horizontal particle layers. The agreement between the measured damping rate and the theoretical value is within 40% for the three highest pressures, but less satisfactory for the lowest.

The data of Fig. 2 are plotted in Fig. 3 in dimensionless form, k/k_D as a function of ω/ω_{pd}. The data nearly coincide in a similarity curve, as would be expected if the dimensionless parameter ν/ω_{pd} were constant, which is nearly so.

The model presented in Eq. (2) is for a homogenous dusty plasma. In the experiment the particles were in a slab only three layers thick. Although the particle motion in both cases is one dimensional, the wave electric fields should have vertical structure in the experiment and not in the model. Nevertheless, the model shows good agreement with the experiment. Fully three-dimensional theories, modeling the particles as a slab of continuum or discrete particles, require numerical techniques, which are now being developed.

The charge ranged from $-3400e$ to $-7200e$, corresponding to a surface potential of -1.05 to -2.20 V with respect to the local dc plasma potential. This is comparable to the charge measured by Trottenberg, Melzer, and Piel [18], who used spheres identical to ours and a similar apparatus. Their experiment differed in using He gas, a higher rf power, and exciting the particle cloud in the vertical direction. The two charge measurement methods differ as follows: Vertical excitation is a disturbance of the cloud's levitation equilibrium, and the analysis requires assumptions about the equilibrium. Horizontal excitation launches a wave, and the analysis requires choosing a theoretical dispersion relation; additionally, it yields λ_D as an output.

The coupling parameters we computed satisfy $\Gamma \gg 1$, indicating the particles were strongly coupled. This conclusion is consistent with the long correlation lengths measured from the static structure. The sharp decline of Γ below 220 mTorr is mostly due to an increase in the dust temperature as the pressure decreases. This transition from low to high T_d was seen by Thomas and Morfill [10] at about the same Kr pressure.

It is striking that a plasma that is strongly coupled according to static measurements obeys a wave dispersion relation that is suitable for a continuum rather than for discrete particles that interact only with their nearest neighbors. Whether this should be attributed to the condition $\lambda_D > \Delta$ in our experiment, or to the WB hypothesis of shielding by the dust particles themselves in the range $\lambda_{Dd} < \Delta$, remains to be determined.

At the present time, our method may be the only practical way of measuring both λ_D and ω_{pd} (i.e., charge). This new capability is needed, but it is tempered by a lack of verification by other means. Calculations of the shielding length and charge based on theoretical models are not practical, since these quantities depend on the ion flow conditions around a grain and plasma non-neutrality in the electrode sheath, which cannot be measured readily.

We thank F. Melandsø and N. Otani for helpful discussions. This work was supported by NASA and NSF.

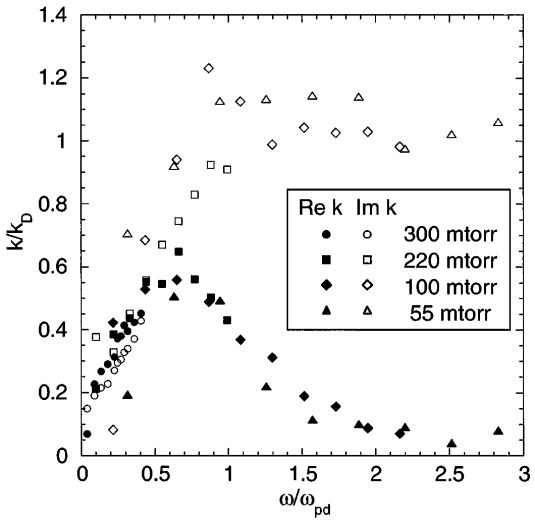

FIG. 3. Experimental data from Fig. 2 scaled by ω_{pd} and $k_D = 1/\lambda_D$. The curves would be expected to coincide if the ratio ν/ω_{pd}, which varies from 0.7 to 1.2, was constant.

*To whom correspondence should be addressed. Electronic address:

[1] C. K. Goertz, Rev. Geophys. **27**, 271 (1989).
[2] N. N. Rao, P. K. Shukla, and M. Y. Yu, Planet. Space Sci. **38**, 543 (1990).
[3] N. D'Angelo, Planet. Space Sci. **38**, 1143 (1990).
[4] F. Melandsø, Phys. Scr. **45**, 515 (1992).
[5] F. Melandsø, T. K. Aslaksen, and O. Havnes, Planet. Space Sci. **41**, 321 (1993).
[6] M. Rosenberg, Planet. Space Sci. **41**, 229 (1993).
[7] H. R. Prabhakar and V. L. Tanna (to be published).
[8] A. Barkan, R. L. Merlino, and N. D.Angelo, Phys. Plasmas **2**, 3563 (1995).
[9] X. Wang and A. Bhattacharjee, Phys. Plasmas **3**, 1189 (1996).
[10] H. M. Thomas and G. E. Morfill, Nature (London) **379**, 806 (1996).
[11] J. B. Pieper, J. Goree, and R. A. Quinn, J. Vac. Sci. Technol. A **14**, 519 (1996).
[12] R. A. Quinn *et al.*, Phys. Rev. E **53**, R2049 (1996).
[13] M. Zuzic, H. Thomas, and G. E. Morfill, J. Vac. Sci. Technol. A **14**, 496 (1996).
[14] Video data from this experiment are available from the server http://dusty.physics.uiowa.edu.
[15] F. Melandsø (to be published).
[16] P. Epstein, Phys. Rev. **23**, 710 (1924).
[17] M. J. Baines, I. P. Williams, and A. S. Asebiomo, Mon. Not. R. Astron. Soc. **130**, 63 (1965).
[18] T. Trottenberg, A. Melzer, and A. Piel, Plasma Sources Sci. Technol. **4**, 450 (1995).